Catastrophic Heat Load on a Solid-Hydrogen Dewar

C.K. Liu,* L.G. Naes,† and A.F. Manikowski Jr.‡
Lockheed Palo Alto Research Laboratories, Palo Alto, California

The cryogenic limb array etalon spectrometer (CLAES) to be launched on board the NASA Upper Atmosphere Research Satellite will utilize a solid-hydrogen tank, insulated by a high-vacuum and multilayer insulation system. Any damage to the vacuum vessel prior to launch is considered catastrophic. As the sudden heat load causes the pressure to rise in the dewar, a burst disk in the emergency vent line will rupture to allow the escape of vaporized cryogenic fluid. For a given vent line system with a given stagnation condition at the inlet, there is a peak flow rate such that the flow will be subsonic throughout the line. Using this peak flow rate, the calculation of the dewar pressure profile depends on an accurate prediction of the dewar heat load. A catastrophic venting test was conducted on a subscale dewar. The test results, which include the effect of the multilayer insulation system and of condensed and/or freezed air layers, were then included in the predicted heat load in the calculation of the CLAES dewar expulsion rate. This heat rate was found to be lower than the predicted peak flow rate and the tank pressure history, after the burst disk rupture, is below the design pressure limits.

Nomenclature

C = specific heat, kJ/kg-K
D = diameter
g = gravitational acceleration, m/s^2
h = heat-transfer coefficient, W/cm^2·K
Δh = heat of transition, kJ/kg
k = thermal conductivity, W/m·K
L = length
$\dot{m}$ = mass flux, kg/s
p = pressure, Pa
$\dot{q}$ = heat flux, W/cm^2
$\dot{Q}$ = total heat load, W
R = thermal resistance
Ra = Rayleigh number
Re = Reynolds number
T = temperature, K
u = internal energy, kJ/kg
v = specific volume, m^3/kg
V = velocity, m/s
x = fraction in Eqs. (17)
Y = free convection parameter defined by Eq. (11), m^{-3}·K^{-1}
β = coefficient of volumetric expansion, K^{-1}
λ = latent heat, kJ/kg
μ = absolute viscosity, kg/m·s
ρ = density, kg/m^3
σ = surface tension

Subscripts

c = condensate
e = efflux
f = liquid
g = gas
H = hydrogen
s = solid
T = total
W = wall

Presented as Paper 85-0960 at the AIAA 20th Thermophysics Conference, Williamsburg, VA, June 19-21, 1985; revision received Nov. 17, 1985.

*Staff Scientist. Member AIAA.
†Research Scientist. Member AIAA.
‡Staff Engineer. Member AIAA.

Introduction

SOLID hydrogen and liquid helium are the only open-cycle systems capable of providing cooling below 15 K. The use of solid hydrogen for spaceborne sensors requiring cryogenic cooling is especially attractive because of the low operating temperature, the high heat of sublimation, and the high specific heat of hydrogen gas. In addition, for those cases where solid hydrogen can be used in place of helium, a substantial weight and volume reduction, by as much as a factor of 10, can be realized.

The NASA Upper Atmosphere Research Satellite (UARS) accommodates 11 instruments, 2 of which are cryogenic instruments. One of these two, the cryogenic limb array etalon spectrometer (CLAES) will utilize a solid-hydrogen (SH_2) cooler for cooling 23 Si(Ga) detectors to less than 15.5 K and the spectrometer optics to less than 25 K. The CLAES cooler is a 944 liter cylindrical tank, insulated for optimal thermal performance by a high vacuum and with a multilayer insulation (MLI) system over the tank surface. Key to the design of the CLAES cryostat is the tank emergency vent system, which must be sized to retain the tank below its design operating pressure of 2 atm differential under the worst case catastrophic event. Since ground tests will be performed with both liquid helium at its normal boiling point and solid hydrogen, the emergency vent system must perform as required for both cryogens. Only the case of hydrogen will be discussed in this paper, although the system has also been analyzed for operation with helium at its normal boiling point.

Two potential accidents are considered critical. These establish the maximum heat flux that the dewar can experience. The first is the damage to the vacuum vessel prior to launch. This condition results in air leaking into the vacuum insulation space, with air condensing on the walls of the solid-hydrogen tank, and represents the maximum credible accident. The second potential accident results from the leakage of hydrogen gas into the vacuum insulation space, which may occur both prior to launch or in space. Heat loads during this type of accident are primarily due to conduction through the gas-filled vacuum space. These heat loads are much lower than those for air leakage and do not dictate the emergency vent line size. Air leakage into the vacuum space is investigated in this analysis, since it is the critical factor establishing vent line sizes.

As the sudden heat load causes the pressure to rise in the dewar, a burst disk in the emergency vent line will rupture at below the tank design pressure differential to allow the

escape of vaporized cryogenic fluid through the emergency vent line system. The latter has to be designed properly such that the expulsion rate of hydrogen is sufficient to keep the pressure below the design pressure limits. In the early stage, there will be liquid expulsion from the dewar. The real concern is when gaseous hydrogen begins to discharge from the dewar. For a given vent line system with a given stagnation condition at the inlet, there is a peak flow rate such that the flow will be subsonic throughout the line. Using this peak flow rate, the calculation of the dewar pressure depends on an accurate prediction of the dewar heat load.

The heat rates incident to the CLAES solid-hydrogen tank during a catastrophic loss of vacuum can be estimated by analytical methods or derived from experimental loss-of-vacuum experiments performed on various liquid-helium dewars. A significant amount of experimental data has been reported by Lehmann and Zahn.[1] The experiments reported in this reference used liquid helium in liquid-nitrogen bath cryostats, both with and without MLI and a liquid-helium transport container with 2 radiation shields and 151 layers of MLI. Measured peak heat rates in these experiments gave an upper limit of about 6.3 W/cm^2 (bare tank) and a lower limit of 0.6 W/cm^2 (transport container). The CLAES solid hydrogen tank will be wrapped with 80 layers (7.6 cm) of double aluminized Mylar and silk net, forming an effective barrier (similar to the transport condition) to heat conduction by air on the CLAES solid-hydrogen tank during a loss-of-vacuum event. Once the peak tank heat rate and flow rate are determined, the pressure history of the CLAES dewar can be determined. A computer program was developed for calculation of the fluid properties in the dewar as a function of time after the rupture of the burst disk.

A catastrophic venting test was also conducted on a subscale dewar to give credence to the analysis. These test results, which include the effect of the multilayer insulation system and of condensed and/or freezed air layers, were then included in the predicted heat load in the calculation of the dewar expulsion rate.

The results show that the predicted peak heat rate of 1.02 W/cm^2 is within the limits of those reported on the liquid-helium dewars.[1,2] The dewar gaseous hydrogen expulsion rate based on the predicted heat load is below the peak flow rates allowed in the proposed emergency vent line system and thus the tank pressures are kept below the design pressure limits.

Sudden Heating of CLAES Dewar

Sudden Heating of Solid-Hydrogen Dewar

At the loss of vacuum, ambient air will leak into the vacuum space insulating the SH_2 dewar. It is assumed that a liquid-nitrogen (LN_2) and/or solid-nitrogen (SN_2) film will form on the cold exterior surface of the dewar, resulting in a sudden heat load to the dewar. The formation of LN_2 and/or SN_2 film and melting of solid hydrogen (SH_2) are complex problems involving transient and spatially dependent simultaneous heat and mass transport in a two- or three-phase mixture that may have one or several components.[3] For practical engineering purposes, a number of reasonable assumptions are necessarily made. Current analysis will cover the events after the loss of vacuum as follows.

When air condenses on the exterior of the dewar wall, the sudden heat load to the dewar will heat the subcooled SH_2 from 10.4 K to the triple point of 13.8 K. This will be followed by an isothermal melting of the SH_2 until the 5% ullage is filled with liquid hydrogen (LH_2). Continuous heating will raise the dewar pressure rapidly to the safety burst disk relief pressure of 0.304 MPa (3 atm). Hydrostatic expulsion of subcooled LH_2 at 13.8 K will then begin through the emergency vent line system. When the SH_2 is completely melted, the dewar will be filled with 13.8 K LH_2. Further heating will raise the temperature of LH_2 to the saturation temperature of 24.62 K corresponding to 0.304 MPa. When this temperature is reached, further heating will evaporate the LH_2. This will begin the expulsion of gaseous hydrogen (GH_2), as the vapor is assumed to accumulate at the top of the dewar where the bellow inlet section of the emergency vent line system is located. Venting of GH_2 will continue until all of the LH_2 has evaporated and until the dewar pressure reaches that of the ambient. The dewar pressure is assumed to remain at 0.304 MPa during the melting of the 13.8 K SH_2 and the evaporation of the 24.62 K LH_2. This is a reasonable assumption as the vent line system designed to handle the peak GH_2 flow is found to be more than adequate to accommodate the LH_2 flow during the SH_2 meltdown. The assumption of these events is based on the following heat-transfer considerations.

The amount of heat required to raise the temperature of SH_2 from 10.4 to 13.8 K is approximately 6.3 kJ/kg. With a predicted total heat load of 48.9 kW (see following section), it takes about 10 s to heat 75.92 kg of SH_2 from 10.4 to 13.8 K. Above 13.8 K, the hydrogen will remain solid only under high pressure, e.g., 6 atm at 14 K and up to the critical point pressure of 12.76 atm at 14.23 K (see Ref. 4, p. 217). Therefore, it is reasonable to assume that all 75.92 kg of the SH_2 will be melted into liquid at 13.8 K. However, due to a 12.3% increase in specific volume from SH_2 to LH_2 at 13.8 K, the volume occupied by 75.91 kg of LH_2 would be 985.54 liters, exceeding the available cryogenic space of 923.7 liters. This implies that the burst disk will be fractured at 3 atm, before the complete melting of the SH_2. Based on the specific volumes of SH_2 and LH_2 of 0.01156 and 0.012983 M^3/kg at 13.8 K, the burst disk will be fractured when 32.46 kg of SH_2 has been melted into liquid and 43.45 kg remains solid. It is assumed here that at this instant, both SH_2 and the slightly compressed LH_2 are maintained at 13.8 K and the density of LH_2 is a function of temperature only. After the complete melting of 75.91 kg of SH_2, there should be 71.15 kg of 13.8 K LH_2 in the dewar. If the excess LH_2 is assumed to be expelled at 3 atm and 13.8 K, the mass of LH_2 expelled with 5% ullage is then 4.76 kg at the end of meltdown. The rate of LH_2 expulsion at 13.8 K is given by

$$\dot{m}_e = \dot{m}_\ell(1 - v_s/v_f) \tag{1}$$

where the second term on right represents the mass of LH_2 occupying the space of melted SH_2. The SH_2 melting rate $\dot{m}_\ell$, based on heat of fusion of 58.29 kJ/kg and a dewar heat load of 48.9 kW, is 0.8387 kg/s. This yields a LH_2 expulsion rate of 0.092 kg/s. Based on the melting rate of 0.8387 kg/s, the fracture of burst disk would occur at 38.7 s after the SH_2 began to melt and total melting takes 90.5 s. At a lower heat load, the melting time will increase accordingly. More sophisticated treatment of the melting process is given in Sec. 3 of Ref. 5.

After the complete melting of the SH_2 at 13.8 K, it can be assumed that LH_2 in the dewar will be rapidly heated from 13.8 to 24.62 K and then evaporate at 3 atm. Any tank pressure fluctuation is not considered at the present time. The heat flux to the LH_2 in the dewar could be calculated between 300 K and T_ℓ of bulk LH_2 with resistances through LN_2 and/or SN_2 and the multilayer insulation (MLI) layers. However, the thickness of SN_2 cannot be estimated with reasonable certainty. Instead, the heat flux is computed between the LN_2 film and LH_2 in the dewar by

$$\dot{q}_T = (77.35 - T_\ell)/R_T \tag{2}$$

The total resistance R_T is the sum of the resistance through the LN_2 film R_c, the dewar wall R_W, and the hydrogen film R_H, viz.

$$R_T = R_c + R_W + R_H \tag{3}$$

The resistance R_c is given by the reciprocal of the LN_2 film condensation coefficient h_c. For a vertical tube,[5]

$$h_c = 0.943\left(\frac{k_f^3\rho_f^2 g\lambda}{L\mu_f\Delta T_c}\right)^{1/4} \tag{4a}$$

and for a horizontal tube

$$h_c = 0.725\left(\frac{k_f^3\rho_f^2 g\lambda}{D\mu_f\Delta T_c}\right)^{1/4} \tag{4b}$$

where

$$\Delta T_c = 77.35 - T_W \tag{4c}$$

The heat flux through the LN_2 film is given by

$$\dot{q}_{N_2} = h_c \cdot \Delta T_c \tag{5a}$$

For the temperature range of interest ($63.15 < T < 77.35$ K), the following relations have been used for the nitrogen condensate film:

$k_f = 0.2462 - 0.001375T_f$, W/m·K

$\rho_f = 1139 - 4.2766T_f$, kg/m^3

$\lambda = 295 - 125T_f$, kJ/kg

$\mu = (1080.4 - 12.295T_f)\times 10^{-6}$, kg/m·s, $64.3 < T_f < 69$ K

$\mu = (882.51 - 9.4286T_f)\times 10^{-6}$, kg/m·s, $69 < T_f < 76$ K

These properties are calculated as functions of the condensate film temperature given by

$$T_f = 77.35 - 0.75\Delta T_c \tag{5b}$$

Values of $\dot{q}_{SN}$ have been calculated using Eq. (5) and plotted in Fig. 1 for T_W between 58 and 67 K. The resistance R_W of the thin metal dewar wall accounts to less than 0.02% of the total resistance and is not considered in the calculations.

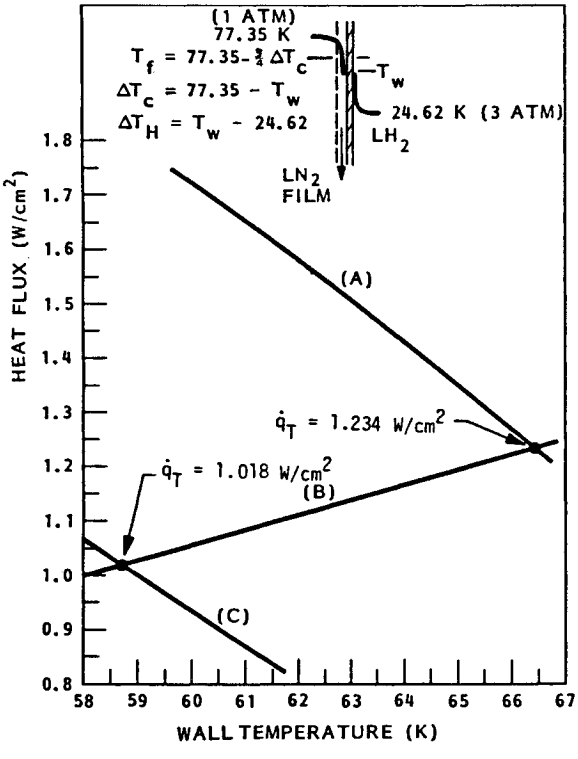

Fig. 1 Peak dewar heat flux [curves A-C from Eqs. (5), (7), and (17), respectively].

The heat flux to the LH_2 in the dewar is a function of the temperature difference $\Delta T_H (= T_W - T_\ell)$. As ΔT_H increases, the initial natural circulation (convection) changes to nucleate boiling. At higher ΔT_H or heat fluxes, more and more nucleation sites becomes active producers of bubbles. A peak nucleate boiling heat flux (called critical heat flux) is reached when bubbles stream forth from so many nucleation sites that the liquid is unable to flow to the heated surface. This is the film boiling where a vapor layer continually blankets the surface. The critical heat flux based on the Kutateladze correlation is given by[5,6]

$$\dot{q}_{cr} = 0.16\cdot\lambda\rho_g^{1/2}[\sigma\cdot g(\rho_f - \rho_g)]^{1/4} \tag{6}$$

At 3 atm, the predicted critical heat flux based on Eq. (6) is 12.7 W/cm^2 at $\Delta T_H = 1.92$ K.

In the present calculation, film boiling is assumed for large ΔT_H. At cryogenic temperatures, the contribution from radiation is neglected and the vapor is generated at the liquid/vapor interface by conduction only. The film boiling data based on the Breen and Westwater correlation[6] may be approximated for ΔT_H of 22-50 K by

$$\dot{q}_{H_2} = 0.0359\Delta T_H^{0.9476} \tag{7}$$

Recent experimental study has found that the heat-transfer coefficient in cases of developed nucleate boiling and film boiling of helium and hydrogen is not affected by subcooling below 2.2 and 12.5 K, respectively.[7] From a given T_f of the LN_2 film, the wall temperature T_W is specified from Eqs. (4c) and (5b). This in turn yields ΔT_H and $\dot{q}_{H_2}$. Values of $\dot{q}_{H_2}$ have thus been calculated and plotted in Fig. 1 for $T_W = 58$-67 K. Since the heat capacitance of the thin dewar wall can be neglected, i.e., $\dot{q}_{N_2} = \dot{q}_{H_2}$, the correct heat flux is given by the interception of the two curves in Fig. 1. This yields a heat flux of $\dot{q}_T = 1.234$ W/cm^2 at $T_W = 66.4$ K. Based on the vent test data (see section on test data comparison), a lower flux of 1.018 W/cm^2 at $T_W = 58.7$ K is used for the present calculations. The total heat load Q_T to the dewar is given by the product of the heat flux $\dot{q}_T$ and the total dewar surface area. The rate of GH_2 expulsion is now given by

$$\dot{m}_e = \dot{m}_g\left(1 - \frac{v_f}{v_g}\right) - \dot{\rho}_g \cdot v_g \tag{8}$$

The last term is the effect on the GH_2 expulsion rate due to rate of change of GH_2 density in the space occupied by GH_2 in the dewar. For a steady flow, this term disappears. The rate of vaporization $\dot{m}_g$ based on $\lambda = 409.78$ kJ/kg at 24.62 K and on the revised heat load of 49 kW, is 0.1193 kg/s. This yields a GH_2 expulsion rate of 0.1126 kg/s at 24.62 K and 3 atm.

As the liquid-hydrogen fraction (LHF) by volume in the dewar decreases, an increasing fraction of the total heat load will be transferred to the GH_2 in the upper portion of the dewar through a natural convection boundary layer. The heat flux to the GH_2 is given by

$$\dot{q}_H = \Delta T_H / R_H \tag{9}$$

where the resistance R_H is given by the reciprocal of the natural heat-transfer coefficient of the GH_2 film h_H, in W/m^2·K. In the turbulent region, h_H is given by[8]

$$h_H = 0.135k_H(Y\Delta T_H)^{1/3}, \quad 10^9 \le R_a < 10^{12} \tag{10}$$

For the bulk GH_2 temperature range of interest ($20 \le T_s \le 60$ K), the following relations have been used for computational purpose:

k_H = thermal conductivity of GH_2 film

$= (-8 + 8.65T_H - 0.025T_H^2)\times 10^{-4}$, W/m·K

where $T_H = T_S + 0.5\Delta T_H$. The free convection parameter Y is defined by

$$Y = \frac{R_a}{L^3 \Delta T_H} = \frac{\beta \rho^2 C_p \cdot g}{\mu k_H} \tag{11a}$$

where $\beta(K^{-1})$, $\rho(kg/m^3)$, $C_p(kJ/kg \cdot K)$, and $\mu(kg/m \cdot s)$ are the coefficient of volumetric expansion, density, specific heat, and absolute viscosity of the GH_2 film, respectively.

If k_H is given in $kW/m \cdot K$, the parameter Y in $m^{-3} \cdot K^{-1}$ is approximated for GH_2 by

$$Y = 4.9712 \times 10^{16} T_H^{-4.2407} \tag{11b}$$

The energy balance on the dewar GH_2 yields

$$\frac{du}{dt} = \frac{v}{V_T}(Q_T - \dot{m}_e \cdot pv) \tag{12}$$

where $\dot{m}_e$ is the mass flow rate of GH_2 out of the dewar. The flow velocity is determined by the mass flow rate $\dot{m}_e$, the specific volume v, and the flow area of the bellow inlet. The value of $\dot{m}_e$ (kg/s) is limited by the peak flow rate in the emergency vent line such that the flow will remain subsonic throughout the line and no choking will occur anywhere in the vent line. This peak flow rate is obtained in an emergency vent line analysis.[9] The rate of change of internal energy from Eq. (12) yields the rate of change of the bulk GH_2 temperature T_s. The mass flow rate $\dot{m}_e$ yields the rate of change of the specific volume v. With the new values of T_s and v given, all other fluid properties in this dewar can be calculated as a function of time.

Computer Program

A program HYGN45 was developed to compute the thermodynamic properties of GH_2 in the dewar as a function of time after the complete evaporation of LH_2.[9] The inputs to this program include values of the peak initial hydrogen flow rate, total area and volume of the dewar, and specific volume of the saturated hydrogen liquid and vapor at a given initial dewar pressure and at a given Teflon bellows inlet diameter. The latter determined the emergency vent line inlet diameter. The program first computes the initial dewar GH_2 mass. The various fluid thermodynamic properties, given two, are evaluated by the general-purpose subroutine PROP[10] and calculated by the substance-specific subroutine PXXX. For a given dewar pressure, the subroutine PROP is used to compute the thermodynamic properties of GH_2 at each increment time after the complete evaporation of LH_2. The subroutine QTHY is used to calculate the heat flux into the dewar GH_2. The computation is carried out until the dewar pressure decreases to 1 atm.

The listed output in HYGN45 includes time, instantaneous dewar GH_2 mass, dewar wall temperature, heat flux to GH_2, GH_2 temperature, pressure, specific volume, Mach number and GH_2 flow rate at the bellow inlet, heat of expulsion, and heat-transfer resistance across the liquid-nitrogen condensation film and hydrogen boundary layer.

Results of Computation

The hydrogen peak flow rates obtained from the emergency vent line analysis[9] are used in the program HYGN45. Table 1 gives the peak flow rate that can be accommodated in the insulated emergency vent line for bellow sizes of 1.91 and 1.59 cm and dewar pressures at 3 and 2.5 atm.

Table 1 Hydrogen peak flow rates in emergency vent lines[8]

Bellow size, cm	$P_s = 3$ atm, kg/s	2.5 atm, kg/s
1.91	0.1833	0.1521
1.59	0.1276	0.1056

A comparison between the hydrogen dewar expulsion rate predicted from Eq. (8) and the peak flow rates from the vent line analysis is given in Fig. 2. The dewar heat load has been revised from 1.234 to 1.018 W/cm^2, yielding a lower melting rate, and resulted in a GH_2 expulsion rate of 0.1126 kg/s. As shown in Fig. 2, the expulsion rates under both heat loads are below the peak flow rate allowable in the emergency vent line system with the 7.94 cm burst disk/check valve and the 1.91 cm bellows.

The properties of GH_2 in the dewar after the burst of disk at 3 and 2.5 atm are obtained from program HYGN45 and are shown in Fig. 3. It shows the pressure and heat flux changes in the hydrogen dewar after complete evaporation. In general, the total time for discharge is proportional to the initial dewar pressure and inversely proportional to the bellow size. There is no pressure buildup in the dewar. The initial value of 0.0678 W/cm^2 to the GH_2 at 3 atm with a 1.91 cm bellow is much lower than the value of 1.018 W/cm^2 to the LH_2 as shown in Fig. 1. The difference is due to the higher resistance of the GH_2 turbulent natural convection layer. The heat flux increases slightly with time at a rate directly proportional to the bellow size.

Catastrophic Vent Test

As mentioned earlier, the calculation of the dewar expulsion rate and the pressure history depends on an accurate prediction of the dewar heat load. The subroutine QTHY that calculates the heat flux to the dewar considers only the effect of the condensed liquid air film, conduction through the aluminum dewar wall, and natural convection inside the dewar. The calculated heat flux is then used to compute the properties of the bulk fluid inside the dewar. Since the thickness of a possible layer of solid air as well as the number of the multilayer insulation layers immersed in solid and liquid air cannot be estimated with reasonable accuracy, a catastrophic venting test was conducted on a subscale dewar. As shown in Fig. 4, the dewar is a 16.51-cm-outside-diam by 22.86-cm-long cylinder of OFHC copper having a wall thickness of 1.27 cm. It was placed in a vacuum vessel with 87 layers of silk net/double-aluminized mylar (DAM) insulation.

Test Summary

A series of five tests was conducted. The first three tests were conducted to check out the system apparatus, instrumentation, and a Hewlett Packard data acquisition system. The test data of the last two tests, one on the cryogen dewar with only a single double-aluminized Mylar (DAM) shield and the other on the dewar with 87 layers of silk net/DAM multilayer insulation (MLI) system were used in the present analysis. Emphasis was placed on the case of the insulated tank, as the

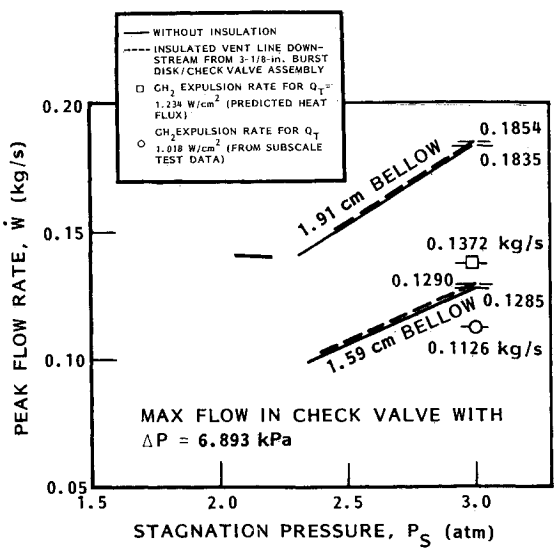

Fig. 2 Peak flow rate vs predicted expulsion rate.

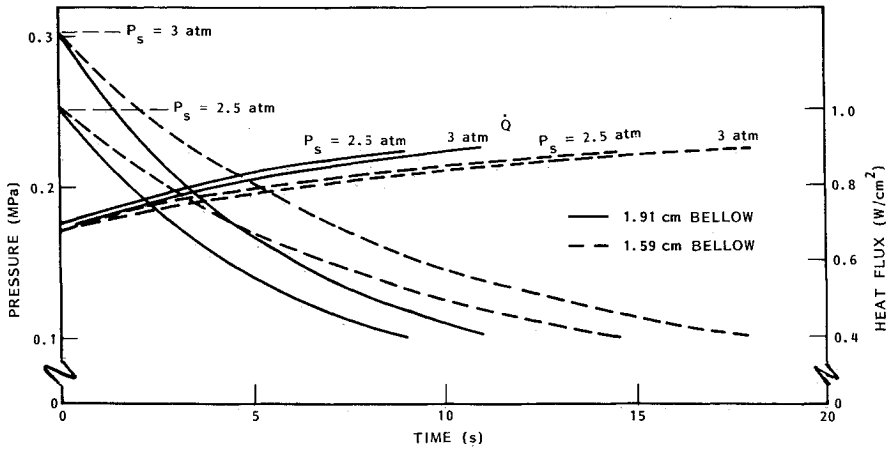

Fig. 3 Dewar pressure and heat flux after burst of disk.

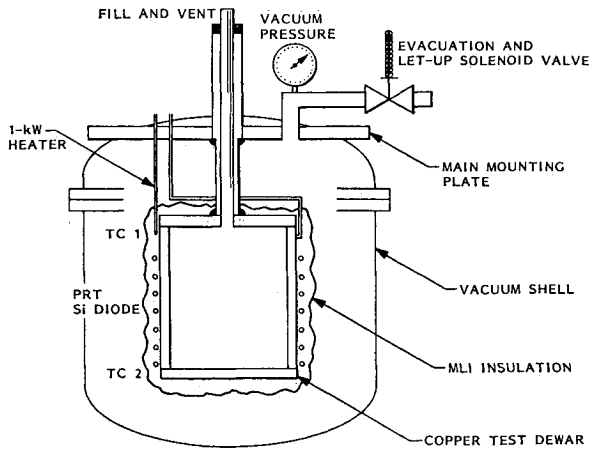

Fig. 4 Schematic of catastrophic vent test apparatus.

CLAES cooler is also to be insulated with a MLI system.

The cryogen dewar was first filled with liquid helium. When the dewar temperature reached equilibrium, the liquid helium was evacuated with a roughing pump and the dewar was sealed off to maintain the vacuum. Ambient air was then let into the insulation vacuum space. As the incoming air condensed and froze on the cold dewar wall surface, the wall temperature rise was monitored by a number of temperature sensors. The weight of the system, including the cryogen dewar, MLI, vacuum shell, and air, was measured with an electronic scale. The change of this total weight was recorded, along with the temperature history of the dewar wall. The heat flux rate was deduced from the rate of temperature rise of the dewar wall, viz.,

$$\dot{Q} = M \cdot C_p \cdot \frac{dT}{dt} \tag{13}$$

where M is the total mass of dewar (15.3 kg) and C_p the specific heat of copper.[11] The average heat flux in W/cm² is given by $\dot{q} = \dot{Q}/A$ where $A = 1614$ cm² is the total exterior surface area of the cryogen dewar. The test results, which include the effect of the multilayer insulation system and condensed and/or frozen air layers, will then be included in the predicted heat load in the calculation of the dewar expulsion rate.

Condensation and Freezing of Air

As the insulation space is being filled with ambient air to 1 atm, it is quite difficult to compute the transient events associated with condensation and freezing of air on a surface at cryogenic temperatures.[2,12] The mechanism of heat transfer through a MLI system containing air, liquid air, and solid air becomes even more complex. In the case of an uninsulated surface at 20 K of various air velocity and temperature, the effect of ambient humidity was investigated in Ref. 2. It was found that low humidity and temperature inhibit and sometimes prevent frost accumulation. With increasing ambient humidity, the frost thickness increases, but the heat-transfer coefficient decreases to a minimum when the frost thickness starts to level off at high values of humidity. The highest heat-transfer rate was found to occur when frost does not accumulate and liquid air flows down the test surface continually. The steady-state heat flux increased from 1.2 W/cm² with 1.2 cm of frost, to 1.8 W/cm² with 0.13 cm of frost, and to 2.5 W/cm² with a thin layer of solid air on the top half of the test surface and running liquid on the remainder of surface. Also, based on the rate of boil-off, heat flux measurements were performed in Ref. 1, on liquid-helium containers with and without superinsulations. The peak heat flux is reduced from 3.8 W/cm² in the former to 0.6 W/cm² in the latter. No analytical model was developed in either cases.

For the purposes of analysis, the present analytical model will consider only the condensation and freezing of nitrogen when air is let into the insulation space. The air rushing into the insulation space will be in a highly turbulent state, at least in the early instants. When the pressure inside reaches 1 atm, there would still be air flowing in or out. The air mass in the dewar insulation space at any instant depends on the nitrogen condensation rate and freezing rate in the early instants, as well as the sublimation rate, melting rate, and evaporation rate during the warmup period. The calculation would usually involve iterations with necessary assumptions based on numerous unknown conditions.

Vapor condensation occurs in two distinct forms. Dropwise condensation occurs only in special cases with the proper combination of vapor and surface conditions. Steam has been found to be the only pure vapor for which conclusive evidence of dropwise condensation is available. The phenomenon more commonly found is the film-type condensation. This is the case to be considered in the present model. During film condensation, the heat transferred at the liquid film surface includes also the superheat of the vapor, in addition to the latent heat of condensation $\dot{q}_{fg}$.

During freezing, the heat generated includes the change in nitrogen enthalpy inside the liquid film $\dot{q}_\ell$ and the heat of fusion at the solid layer surface $\dot{q}_{sf}$. When the cryogen dewar wall temperature is below 35 K, the heat generated also includes the change in enthalpy of solid nitrogen due to the alpha-gamma transition $\dot{q}_{ag}$ in addition to cooling of solid nitrogen $\dot{q}_s$.

The rate at which the heat is generated, in W/cm², is given by

$$\dot{q}_{fg} = \Delta h_{fg} \cdot \dot{m}_c \tag{14a}$$

$$\dot{q}_\ell = m_\ell \cdot C_\ell \cdot \Delta T_c / 2 \tag{14b}$$

$$\dot{q}_{sf} = \Delta h_{sf} \cdot \dot{m}_F \tag{14c}$$

$$\dot{q}_s = \dot{m}_F \cdot C_S \cdot (63.15 - T_W)/2 \tag{14d}$$

$$\dot{q}_{ag} = \Delta h_{ag} \cdot \dot{m}_F \tag{14e}$$

$$\dot{q}_M = M_M \cdot C_M \cdot \Delta \dot{T}_M \tag{14f}$$

where $\dot{m}_c$ and $\dot{m}_F$ are rate of condensation and freezing per unit surface area (g/cm^2·s), $\dot{m}_\ell$ the average mass flux of liquid nitrogen per unit width of liquid film (g/cm^2·s), C_ℓ the specific heat of liquid nitrogen at T_f, and C_s the specific heat of solid nitrogen at $(63.15-T_W)/2$. The heat released to cool the MLI layers embedded in liquid and solid nitrogen, $\dot{q}_M$, can be estimated only by assumptions of the number of layers embedded in nitrogen and $\Delta\dot{T}_M$ from rate of dewar temperature change. The thermodynamic properties are given in Table 2.

The values of $\dot{m}_c$, $\dot{m}_\ell$, and $\dot{m}_F$ cannot be directly computed from the ambient air ingestion rate, particularly with the presence of the MLI system. However, the values may be estimated from the weight change monitored during the tests in each temperature range. The specific heats and mass of the MLI layers embedded in nitrogen are so low that for practical purpose, $\dot{q}_M$ can be neglected in the analytical model without any significant effect on the results.

Table 2 Thermodynamic properties

$\Delta h_{fg}=199.15$ J/g at 77.35 K
$\Delta h_{sf}=51.47$ J/g at 63.15 K
$\Delta h_{ag}=16.34$ J/g at 35.6 K
$C_\ell=2.03$ J/g·K at 70 K
$C_s=1.36$ J/g·K at 40 K
$C_M=0.356$ J/g·K at 70 K
$=0.21$ J/g·K at 40 K

Heat Flux Predictions

The heat-transfer mechanisms will be examined below and an attempt will be made to find the most realistic approach for predicting the heat flux into the cryogen dewar. When the insulation space is filled with air, the heat flow from the vacuum shell to the cryogen dewar wall (vertical side) is shown in Fig. 5. The heat flux in W/cm^2 can be estimated by

$$\dot{q}_A=(300-T_M)/R_A \tag{15a}$$

$$\dot{q}_M=(T_M-77.35)/R_M \tag{15b}$$

$$\dot{q}_{LN}=(77.35-63.15)\Big/\left[\left(\frac{1}{N_L\cdot R_{Net}}+\frac{1}{R_{LN}}\right)^{-1}+N_L\cdot R_{DAM}\right] \tag{15c}$$

$$\dot{q}_{SN}=(63.15-T_W)\Big/\left[\left(\frac{1}{N_S\cdot R_{Net}}+\frac{1}{R_{SN}}\right)^{-1}+N_S\cdot R_{DAM}\right] \tag{15d}$$

where T_M and T_W are the temperature of the outermost layer of the MLI and that of the dewar wall, respectively. The latter has been measured in the tests, but T_M is not known. The resistance R_A, assuming stationary air, is given by X_A/k_A, where X_A is the thickness of the air gap betwen the vacuum shell and MLI. Atmospheric air has a relatively high thermal conductivity near room temperature.[13] Preliminary calculations with $X_A=7$ cm (see Fig. 5) yielded values of T_M very close to the room temperature.

The resistance R_M depends on the thickness and number of layers of the 3.18 cm, 87 layer MLI system not occupied by liquid and solid nitrogen, as well as the MLI thermal conductivity. The thermal conductivity of MLI in vacuum is given by the first term in Eq. (2) of Ref. 14. As the pressure increases to 1 atm, the thermal conductivity of the silk-net/DAM MLI system approaches that of the nitrogen gas.[15]

The resistance of a single silk-net spacer and a single DAM is given by their conductivity and thickness (0.1016 mm of silk-net and 0.00635 mm of DAM). However, calculations of $\dot{q}_{LN}$ and $\dot{q}_{SN}$ depend also on the number of silk-net/DAM shields, N_L and N_S, embedded in the liquid- and solid-nitrogen layers.

The thermal resistance of the liquid-nitrogen film R_{LN} is given by the reciprocal of the liquid-nitrogen condensation coefficient h_c computed from Eq. (4). The resistance of the solid-nitrogen layer R_{SN} is given by X_{SN}/k_{SN}, where X_{SN} is the thickness of the layer estimated from the measured weight increase, the total exterior surface area of the cryogen dewar, and the density of the solid nitrogen, i.e.,

$$X_{SN}=\frac{\Delta W}{\rho_{SN}\cdot A} \tag{16}$$

It is assumed that the nitrogen freezes at a temperature below 63 K. Hence, the density and thermal conductivity of solid nitrogen are assumed to be 0.562×10^{-3} kg/m^3 and 0.39 W/m·K, respectively.[16]

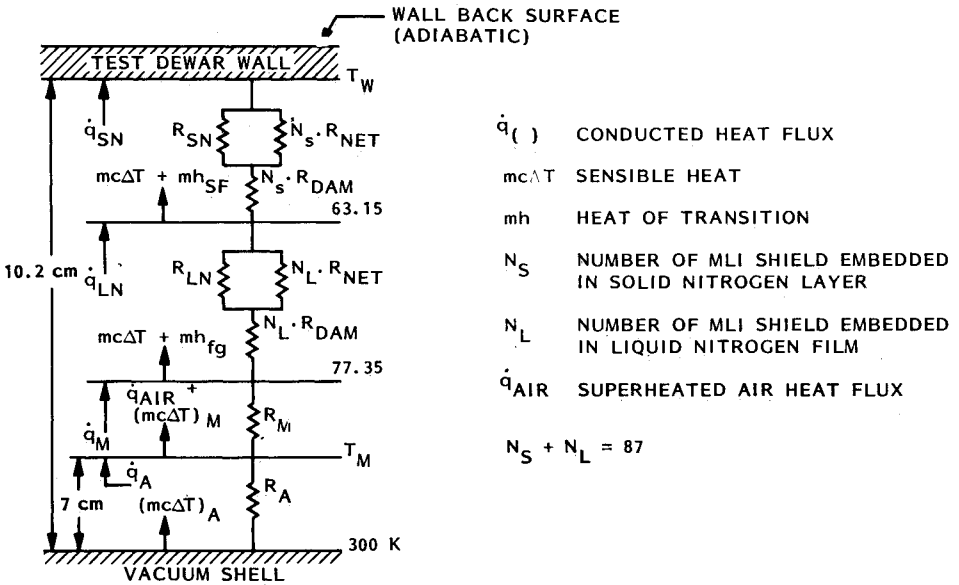

Fig. 5 Path of heat flow in subscale dewar test. ($\dot{q}_{(\ )}$ = conducted heat flux, $mc\Delta T$ = sensible heat, mh = heat of transition, N_S = number of MLI shield embedded in solid-nitrogen layer, N_L = number of MLI shield embedded in liquid-nitrogen film, $\dot{q}_{air}$ = superheated air heat flux.)

Table 3 Thermal resistances

Components	Thermal resistance, $m^2 \cdot K/W$ 40 K	70 K
R_{DAM}	8.6×10^{-5}	6.6×10^{-5}
R_{Net}	1.7×10^{-2}	2.8×10^{-2}
R_{LN}		6.6×10^{-4}
R_{SN}	$1.1\text{-}3\times10^{-3}$	

Table 4 Heat of transition and sensible heat, W

	Bare tank test	Insulated tank test
q_{ag}	–	445
q_{sf}	646	315
q_{fg}	645	650
q_s	–	165
q	50	110

Since X_A and X_M cannot be estimated with reasonable certainty, Eqs. (15a) and (15b) will not be used. Instead, Eq. (15c) will be used for the heat flux calculation for T_W above 63.1 K. At lower T_W, Eq. (15d) is used with X_{SN} estimated by use of Eq. (16).

The thermal resistances are computed at 40 K (inside the solid-nitrogen layer) and 70 K (inside the liquid-nitrogen layer) for various components in Table 3.

It is seen that values of R_{Net}, in parallel with R_{LN} and R_{SN}, in Eqs. (15c) and (15d) are at least two and one orders of magnitude higher than that of R_{LN} and R_{SN}, respectively. Hence, they are neglected in further heat flux calculations. The value of R_{DAM}, in series with R_{LN} and R_{SN}, is small, but the total resistance (depending on N_L and N_S) may not be neglected. The thickness (or mass) of the liquid- and solid-nitrogen layers is not known and cannot be estimated with any reasonable certainty. This makes it difficult to estimate the number of DAM, N_L, and N_S, embedded in the liquid- and solid-nitrogen layers.

The current approach is to utilize the measured dewar wall temperature as the cold boundary. It is also assumed that the measured total weight increase in the early instants (before the dewar wall temperature rises to 63 K) represents mainly the amount of solid nitrogen on the dewar wall. The heat flux is calculated without the R_{Net} and R_{DAM} terms by use of Eq. (15c) for T_W above 63.1 K and Eq. (15d) for lower T_W. An estimated fraction is then deducted from the heat flux to account for the effect due to the DAM resistance, the nitrogen heats of transiton (alpha/gamma transition of solid nitrogen at 35.6 K, solid/liquid nitrogen transition at 63.15 K, and liquid/vapor nitrogen transition at 77.35 K), the sensible heat required to warm the various components to yield the heat flux that finally enters the cryogen dewar wall.

Comparison with Test Data

The heat flux to the dewar wall is calculated from Eqs. (15c) and (15d), reduced by the estimated values of heat of transition and sensible heat. The latter are calculated from Eq. (14) and the values are given in Table 4.

In the bare tank (with single DAM shield) test, the dewar wall temperature has risen to 46.6 K when air was let in. Hence, no values of $\dot{q}_{ag}$ and $\dot{q}_s$ are computed. The measured temperature data are those of the Chromel-Constantan thermocouples located at the top and bottom of the dewar side (see Fig. 4). The dewar wall temperature rose from 46.6 K when air was let in, to 62.7 K after 7 s and to 76.8 K after 42 s. The corresponding weight changes were 87.86 and 136 g.

The total heat flux computed from Eq. (13) agrees with that from Eqs. (15c) and (15d) if the assumption is made that 25% of the $\dot{Q}_{LN}$ computed from Eq. (15) be assigned to heat of transition and sensible heat and 75% of the $\dot{Q}_{LN}$ enters the dewar wall after the first 4 s when the wall temperature soon rose above 60 K and the solid-nitrogen layer began to melt completely. In the first 4 s, it may be assumed that no adjustment for the heat of transition is needed.

Of more practical importance is the result from the insulated tank test. The dewar wall temperature rose from 26.4 K (vs 46.6 K in bare tank test) when air was let in, to 63 K after 23 s and 74.6 K after 60 s. The corresponding weight changes were 114 and 196 g. The total heat flux computed from Eq. (13) is shown in circles in Fig. 6. It shows wider fluctuations with time than that in the bare tank test. The trends of the data points between the nitrogen transition temperatures (35.6 and 63.15 K) in Fig. 6 do not show any consistency to offer any plausible explanation at the present time. The effect due to the oxygen heat of fusion (13.8 J/g at 54.3 K) should be small.

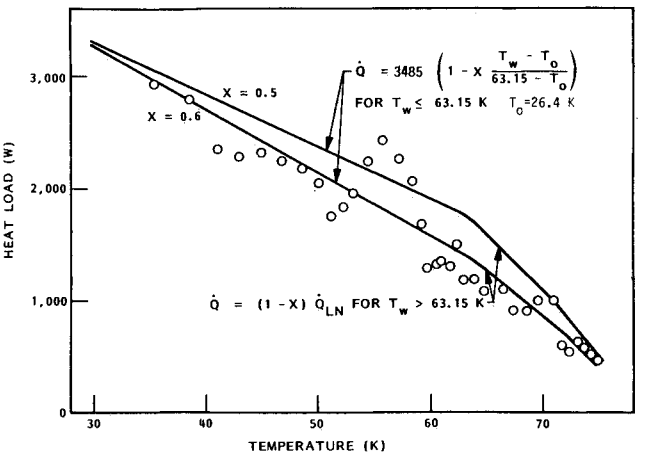

Fig. 6 Heat load from insulated tank test.

For a temperature difference between 77.35 and 63.15 K across the liquid-nitrogen film, the heat flux $\dot{Q}_{LN}$ based on Eq. (15c) is 3485 W. The total heat flux prediction, based on wall temperature data, seems to agree generally well with the test data if the following equations are used:

$$\dot{Q}_W = 3485\left(1 - x\frac{T_W - T_0}{63.15 - T_0}\right), \qquad T_W \leq 63.15 \text{ K} \quad (17a)$$

$$\dot{Q}_W = (1-x)\cdot\dot{Q}_{LN}, \qquad T_W > 63.15 \text{ K} \quad (17b)$$

The value of x is close to 0.5 in Fig. 6, with reasonable agreements between the heat flux computed from Eqs. (13) and (17). The higher percentage of deduction in the insulated tank test is due to lower initial wall temperature resulting from the MLI system. The deduction includes the additional heat of transition of 35.6 K as well as the larger amount of heat required to cool the solid nitrogen to the lower wall temperatures.

Conclusions

A comprehensive heat-transfer analysis is not possible with the information available at the present time. The analytical model developed in the current analysis involves a number of assumptions on the effects of the MLI resistance and the cryodeposit, the heats of transition, and the sensible heat. This is unavoidable in the absence of sufficient information on the rate of ambient air condensation, freezing, sublimation, melting, and evaporation. Nevertheless, some conclusions may be drawn from the analysis for the prediction of the heat flux to a cryogen dewar:

1) A simple heat-transfer analysis would neglect the heats of transition and sensible heats, i.e.,

$$\dot{Q}_{N_2} = \dot{Q}_W = \dot{Q}_{H_2}$$

2) The predicted heat flux to the cryogen would be overly conservative. On the bare tank with a single DAM shield, catastrophic heat flux prediction may be made as a function of surface temperature if a fraction of the heat flux computed from Eq. (5) is assigned to the heats of transition and the sensible heats. This fraction is zero in the first 4 s before the wall temperature reaches 60 K and 25% thereafter.

3) On the insulated tank, a similar prediction may be made if $x = 0.5$ is used in Eq. (17). This prediction could be on the conservative side.

More insight into the mechanism of heat transfer through a multilayer insulation containing air in different phases has been gained in the present analysis. The analytical model developed here will be useful in a more accurate assessment of the heat flux into the insulated CLAES solid-hydrogen cooler during the loss of vacuum. This will in turn yield a more realistic sizing of the emergency venting system.

References

[1]Lehmann, W. and Zahn, G., "Safety Aspects of Liquid Helium Cryostats and Liquid Helium Transport Containers," *Proceedings of Seventh International Cryogenic Conference,* London, July 1978, pp. 569-579.

[2]Van Gundy, D.A. and Uglum, J.R., "Heat Transfer to an Uninsulated Surface at 20 K," *Advances in Cryogenic Engineering,* Vol. 7, Plenum Press, New York, 1962, pp. 377-384.

[3]Contreas, W. and Lee, M., "Melting Characteristics and Bulk Thermophysical Properties of Solid Hydrogen," AFRPL-TR-72-48, July 1972.

[4]McCarty, R.D., "Hydrogen Technology Survey—Thermophysical Properties," NASA SP-3089, 1975.

[5]Rohsenow, W.M., and Hartnett, J.P. (eds.), *Handbook of Heat Transfer,* McGraw-Hill Book Co., New York, 1973.

[6]Kutateladze, S.S., *Fundamentals of Heat Transfer Theory,* M. Atomizdat, Moscow, 1979.

[7]Kirichenko, Yu. A., Rusanov, K.V., and Tyurina, E.G., "Heat Transfer in Subcooled Liquid Cryogens," *Cryogenics,* Vol. 23, April 1983, pp. 209-211.

[8]McAdams, W.H., *Heat Transmission,* McGraw-Hill Book Co., New York, 1975.

[9]Liu, C.K., "Safety Analysis of Modified CLAES Dewar and Emergency Vent Line Systems," Lockheed Missiles and Space Co., Palo Alto, CA, Rept. EM E84-009, Oct. 1984.

[10]Reynolds, W.C., "Thermodynamic Properties in SI," Dept. of Mechanical Engineering, Stanford University, Stanford, CA, Jan. 1979.

[11]Childs, E.G., Ericks, L.J., and Powell, R.L., "Thermal Conductivity of Solids at Room Temperature and Below," National Bureau of Standards, Washington, DC, Monograph 131, Sept. 1973.

[12]Van Gunday, D.A., "Establishing Tank Design Criteria for Liquid Hydrogen Rockets, Vol. II: Heat Transfer to Liquid Hydrogen through Condensing Air Films," AFFTC TR-60-43, Beechcraft Engineering Rept. 8768, July 1, 1961.

[13]Johnson, V.J., "A Compendium of the Properties of Materials at Low Temperature (Phase 1), Part I: Properties of Fluids," WADD TR-60-56, Pt., I, July 1960.

[14]Bell, G.A., Nast, T.C., and Wedel, R.K., "Thermal Performance of Multilayer Insulation Applied to Small Cryogenic Tankage," *Advances in Cryogenic Engineering,* Vol. 22, Plenum Press, New York, 1977, pp. 272-282.

[15]Coston, R.M., "Handbook of Thermal Design Data for Multilayer Insulation Systems, Final Report," *High Performance Insulation Thermal Design Criteria,* Vol. II. NAS 8-20353, LMSC-A847882, June 1967.

[16]Cook, T. and Davey, G., "The Density and Thermal Conductivity of Solid Nitrogen and Carbon Dioxide," *Cryogenics,* Vol. 16, 1976, p. 363-369.